



ELSEVIER

Surface Science 364 (1996) L631–L637

surface science

Surface Science Letters

# Monochromatization of atomic waves by nanoscopic echelette gratings

Hansjörg Schief, Vittorio Marsico, Klaus Kuhnke, Klaus Kern \*

*Institut de Physique Expérimentale, Ecole Polytechnique Fédérale de Lausanne, CH-1015 Lausanne, Switzerland*

Received 25 March 1996; accepted for publication 30 April 1996

## Abstract

The vicinal Pt(997) surface is introduced as a high-performance nanoscopic reflection grating (echelette grating) for atomic waves. Its atom-optical properties with respect to thermal He beams are established by a detailed high-resolution diffraction study. The absolute efficiency of the Pt(997) echelette grating has been measured to vary between 2 and 20% depending on the He wavelength. In a double surface-scattering experiment the nanoscopic echelette grating has been used for active monochromatization of He atom waves down to  $\Delta\lambda/\lambda=0.6\%$ .

*Keywords:* Atom–solid scattering and diffraction – elastic; Platinum; Vicinal single crystal surfaces

Atom optics is currently becoming an exciting new field in fundamental physics [1]. The term refers to experimental techniques to realise optical elements for neutral atom and molecular beams (e.g. mirrors, beam splitters, gratings) by either directly manipulating the particle trajectories or by taking advantage of the de-Broglie wave properties of the beams. Diffraction of atomic and molecular de-Broglie waves was, however, already being used systematically in surface science long before the term “atom-optics” came into vogue [2,3]. In this Letter we focus on the application of surface diffraction as an active atom-optical device. In particular we will demonstrate that surface diffraction from nanoscopic echelette gratings can be used for an efficient active monochromatization of He atom waves.

The success of diffractive atom optics employed

in molecular beam experiments depends crucially on the quality of the corresponding diffraction gratings. Despite the recent success in the fabrication of free-standing transmission gratings (such as Fresnel zone plates [4] or line gratings [5]), surface diffraction is the most promising way to realise high-performance diffraction gratings. Historically the alkali halide single-crystal surfaces have been used as diffraction gratings [2,6]. Due to their high corrugation, these surface gratings have the disadvantage of numerous open diffraction channels distributing the diffracted intensity into many directions. An ideal surface diffraction grating used as monochromator or analyser would reveal only a few open diffraction channels, in order to obtain enhanced reflectivity in higher-order diffraction peaks. In classical light optics this is achieved by stepped reflection gratings, i.e. blazed or echelette gratings [7]. They consist of flat terraces with an almost perfect reflectivity,

\* Corresponding author. Fax: +41 21 6933604.

separated by steps which are much smaller than the terrace width.

Knowing about the performance of echelette gratings in classical optics, it becomes desirable to transfer this concept to atom-optics dealing with wavelengths of the order of 1 Å. Since the grating period must scale with the wavelength, this would require the fabrication of stepped gratings in the 1 nm range, which exceeds current technologies. But nature provides a class of crystal surfaces (i.e. regularly stepped surfaces with close-packed terraces) which can be used directly as nanoscopic echelette gratings [8,9]. An example of such a surface is the vicinal Pt(997) surface, consisting of (111) terraces about 20 Å wide separated by (11 $\bar{1}$ ) monatomic steps (Fig. 1a). This surface combines the high specular He-reflectivity of the Pt(111) surface [10] with the required step-terrace arrangement of a blazed grating. Comsa et al. [8] demonstrated in their pioneering He-diffraction study, that this surface essentially acts as an echelette grating. In Fig. 1b we show an STM image of the well-prepared Pt(997) surface, nicely confirming the regular step-terrace ordering which is essential for its use as nanoscopic blazed grating; a detailed account of the STM work can be found in Ref. [9].

The He atom diffraction experiments reported here have been performed with a novel He-surface double axis spectrometer [11,12], consisting of a He nozzle beam source ( $\Delta\lambda/\lambda \approx 1\%$ ), a target chamber containing the Pt(997) surface and an analyser/detector set-up containing the analyser surface (either a second Pt(997) surface or a Pt(111) surface as a simple mirror). Both metal surfaces are prepared, maintained and manipulated in UHV. Angular movements of the analyser crystal and of the whole analyser/detector assembly can be controlled with an absolute precision better than 0.005°.

He diffraction from periodic surfaces is described by the product of a structure factor  $G^2$  and a form factor  $A^2$

$$I \sim A^2 G^2. \quad (1)$$

The form factor describes the diffraction from the unit cell. In our case of He diffraction from a vicinal surface, the form factor  $A^2$  can be expressed

in terms of the simple optical model for diffraction from echelette gratings [7,8]. It corresponds to simple specular scattering from the finite (111) terraces:

$$A^2 = \frac{\sin^2 \frac{\phi}{2}}{\left(\frac{\phi}{2}\right)^2}, \quad (2)$$

$$\phi = \frac{2\pi}{\lambda} \tilde{D} [\sin(\vartheta_i - \alpha) - \sin(\vartheta_r + \alpha)].$$

Here,  $\vartheta_i$  and  $\vartheta_r$  are the angle of incidence and the scattering angle with respect to the macroscopic surface normal,  $\alpha$  denotes the angle between the macroscopic surface and the close-packed (111) terraces, and  $\tilde{D}$  is the effective terrace length as seen by the He wave.  $\tilde{D} < D$  (with  $D$  being the nominal step-step distance) accounts for the fact that the He wave sees only an effective terrace width due to the shadowing of the step edge and the diffuse step edge scattering [11,13]. The structure function  $G^2$  describes the interference between terraces and is given by the one-dimensional Bragg condition

$$G^2 = \sum_n \delta \left( \sin \vartheta_r - \sin \vartheta_i - \frac{n\lambda \cos \alpha}{D} \right). \quad (3)$$

For each angle of incidence the positions of the diffracted beams are given by the structure function Eq. (3); their intensities are determined by the form factor Eq. (2). Variation of the angle of incidence leads to a continuous shift of the positions of the diffracted beams with respect to the specular direction of the terraces. Thus, the maximum of the form factor  $A^2$  can be made to coincide with a higher-order diffraction peak by a suitable choice of the angle of incidence. Under this in-phase scattering condition with respect to adjacent terraces almost the total reflected intensity is concentrated in one single higher-order diffraction peak.

The proof that Pt(997) is acting as nanoscopic echelette grating is given in Fig. 1c, where we show three typical He diffraction spectra obtained with an He wavelength  $\lambda = 0.959$  Å by varying the total scattering angle ( $\vartheta_i + \vartheta_r$ ) at a fixed angle of incidence. The curves on the left and right-hand sides

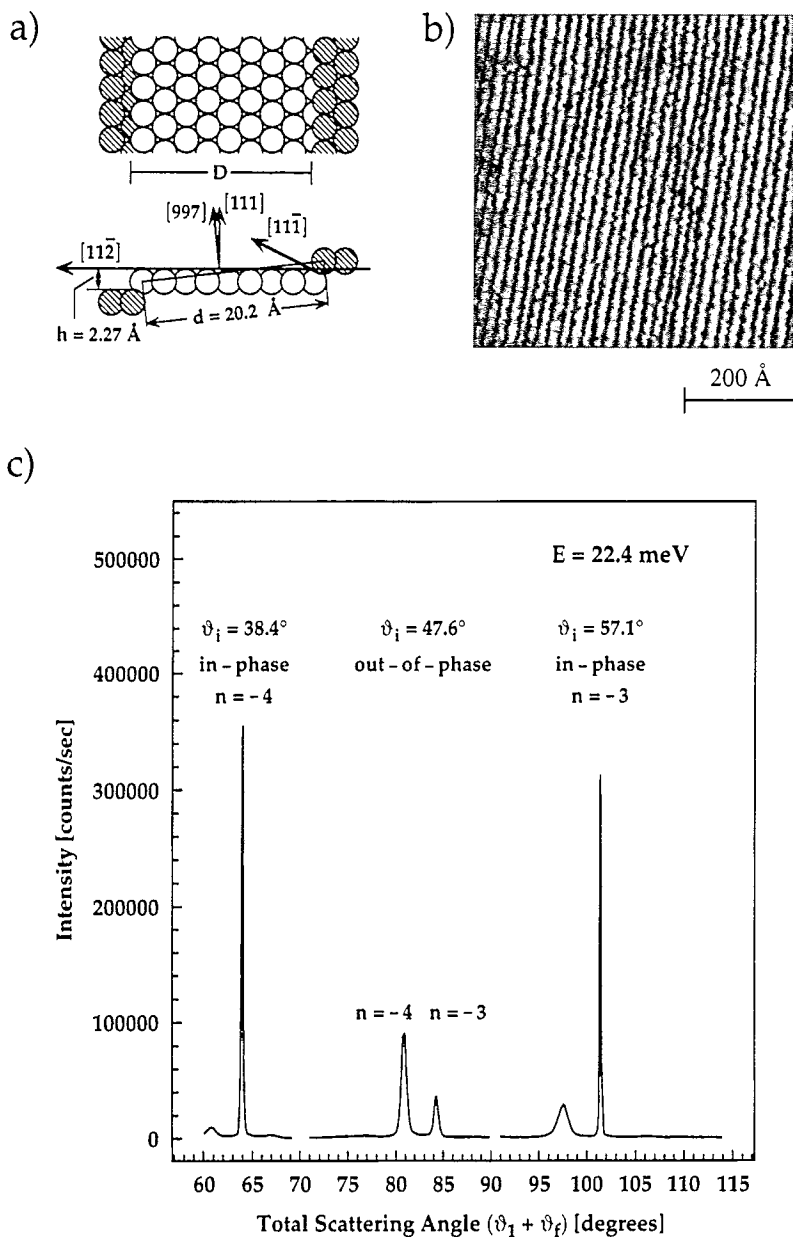


Fig. 1. (a) Schematic top- and side-view of the Pt(997) surface. (b) STM image of the clean, well-prepared Pt(997) surface. (c) High-resolution He diffraction scans from Pt(997) (beam energy 22.4 meV,  $\lambda = 0.959 \text{ \AA}$ ).

correspond to the in-phase scattering conditions of the  $n = -4$  and  $n = -3$  diffraction orders, respectively (the negative sign indicates scattering in the step-down direction). In agreement with the optical model for diffraction from stepped reflection gratings, the spectrum is dominated by one intense

and very sharp ( $0.12^\circ$  FWHM) diffraction peak, i.e. almost all the diffracted intensity is concentrated in one channel. The spectrum in the middle, on the other hand, has been obtained at an out-of-phase scattering condition, leading to the appearance of two diffraction orders which are less

intense than in the in-phase condition. This is again in full agreement with the optical model. The main deviation from the optical model is the diffraction-peak broadening observed under out-of-phase conditions. It is due to the finite terrace width distribution of the Pt(997) surface, as revealed by our recent STM study [9].

However, this disadvantageous influence of grating irregularities is absent in the above-mentioned in-phase scattering condition. More precisely, our detailed experimental and theoretical study reveals that the peak broadening does not significantly affect the resolving power of the Pt(997) grating, only if the in-phase scattering condition is maintained within an error of the order of  $0.05^\circ$ . The wavelength separation of the nanoscopic echelette grating for in-phase diffraction is given by

$$\frac{\Delta\lambda}{\lambda} = \frac{1}{2} \left[ \frac{D}{h} + \tan(\vartheta_f + \alpha) \right] \Delta\vartheta, \quad (4)$$

with  $h=2.27 \text{ \AA}$  being the step height. Thus,  $\Delta\lambda/\lambda$  depends only slightly on the wavelength and the diffraction order, since  $\tan(\vartheta_f + \alpha)$  is in practical cases much smaller than  $D/h = \cot(\alpha) = 8.9$ . However, it depends linearly on the angular resolution of the experimental geometry  $\Delta\vartheta$  [14]. In the out-of-phase condition, the peak broadening due to terrace-width irregularities adds to the diffraction-peak width, and can easily become the dominant term. This is demonstrated in Fig. 2 which shows the measured excess FWHM due to the finite terrace distribution obtained in the very close vicinity of the  $n = -3$  in-phase condition. A deviation of  $0.1^\circ$  from the ideal condition gives rise to an extra broadening of about  $0.02^\circ$ . Only for deviations less than  $0.05^\circ$  is the extra broadening negligible.

An important criterion for the suitability of nanoscopic blazed gratings is their efficiency, i.e. the amount of collected intensity within one higher diffraction order with respect to the incoming flux (Fig. 3). Depending on the wavelength and the diffraction order, the measured efficiency varies between 2 and 16% (most recently we have reached up to 20% at  $\lambda = 0.959 \text{ \AA}$ ,  $n = -4$ ). The efficiency of the Pt(997) echelette grating is thus at least one order of magnitude higher than that of any low-

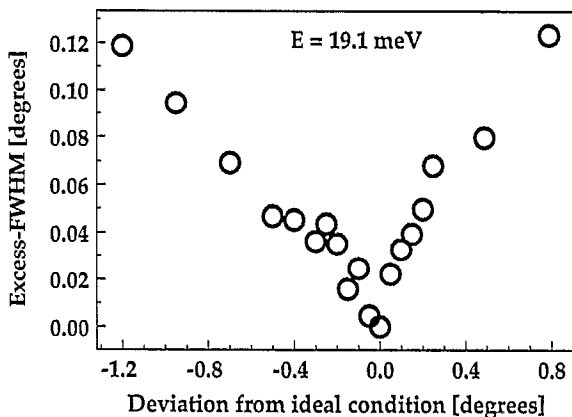


Fig. 2. Excess FWHM due to the finite terrace width distribution obtained in the very close vicinity of the  $n = -3$  ideal diffraction condition with a 19.1 meV beam ( $\lambda = 1.039 \text{ \AA}$ ). The data are plotted as a function of the deviation from the ideal in-phase condition.

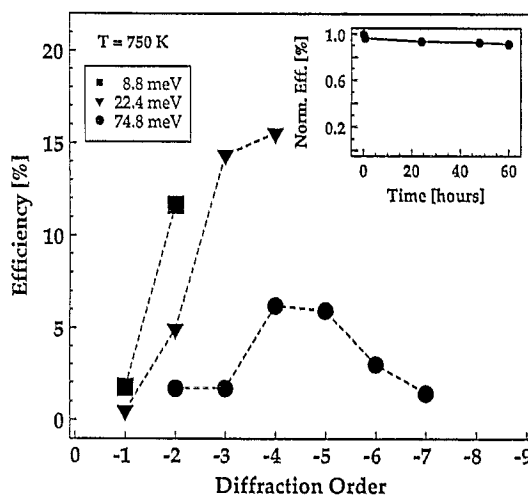


Fig. 3. Absolute efficiencies of Pt(997) for He diffraction in the ideal in-phase conditions for wave lengths of  $1.53 \text{ \AA}$  (8.8 meV),  $0.959 \text{ \AA}$  (22.4 meV) and  $0.525 \text{ \AA}$  (74.8 meV). The inset shows the temporal variation of the normalized absolute efficiency ( $E = 22.4 \text{ meV}$ ,  $n = -4$ ) during operation in the autocatalytic cleaning mode (see text).

index crystal surface (in non-specular diffraction). There are two important trends seen in Fig. 3. First, for a given diffraction order, the efficiency increases substantially with increasing wavelength (i.e. decreasing energy). Second, at a given wavelength, the efficiency increases with increasing

diffraction order  $|n|$ . The first effect is mainly due to the Debye–Waller effect: the reflectivity decreases with beam energy because the probability for inelastic processes increases. The second trend is due to the geometrical shadowing effect which is dominant at low diffraction orders (large  $\vartheta_i$ ) and loses importance with increasing  $|n|$ . The Debye–Waller attenuation and the shadowing effect work in opposite directions, which is the reason for the maximum in the Efficiency– $n$  curve for  $\lambda=0.525$  Å.

The efficiency and all other atom-optical properties of Pt(997) have been measured at a fixed temperature of 750 K. At this temperature a permanent auto-catalytic cleaning procedure has been developed in order to provide a reliable long-time and comfortable use of the Pt(997) surface under standard UHV conditions. The surface is kept permanently at an oxygen partial pressure of  $5.0 \times 10^{-9}$  mbar. Thus, carbon impurities are oxidised to desorbing CO. On the other hand, the build-up of an oxygen coverage is prevented by a simultaneous exposure of the surface to a hydrogen atmosphere of  $5.0 \times 10^{-7}$  mbar, leading to the formation of desorbing water. The performance of this passivation has been checked by measuring the absolute efficiency as a function of time (see inset in Fig. 3). Neither an important contamination nor a morphological change of the surface occurs upon the surface passivation described above. The Pt(997) surface can routinely be used for several weeks without any significant intensity loss and without further surface preparation.

Having established the diffraction properties of the Pt(997) surface with respect to thermal He atoms, we have employed it as a nanoscopic echellette grating for the active monochromatization of He waves. Apart from the pioneering work of Stern and co-workers in 1931 [15] the experiments discussed below are the only demonstration so far of active monochromatization of atomic de Broglie waves by diffraction. Eq. (4) has shown that the wavelength resolution of the echellette grating varies linearly with the geometrical angle spread  $\Delta\vartheta$ . Monochromatization can thus be very easily achieved by restriction of  $\Delta\vartheta$ , i.e. by placing adequate apertures in front of and behind the Pt(997) monochromator. Fig. 4a shows schematically the

scattering geometry used in our monochromatization experiments. A slightly polychromatic primary He beam ( $\Delta\lambda/\lambda > 1.3\%$ ) is scattered off the Pt(997) monochromator. Atoms with different wavelengths are diffracted into different directions. The aperture behind the monochromator skims a wavelength-selected beam ( $\Delta\lambda/\lambda = 0.006$  for the particular geometry) which is then analysed by high-resolution analyser diffraction scans. As the analyser crystal we have either used a Pt(111) surface covered with a  $p(2 \times 2)$  oxygen overlayer [16] or a second Pt(997) surface. Monochromatization is demonstrated by comparing diffraction spectra from the analyser surface taken with and without monochromatization. For the  $p(2 \times 2)\text{O}/\text{Pt}(111)$  analyser surface we have used the half-order diffraction peak, while with the Pt(997) analyser we have used the  $n = -3$  in-phase condition. In both cases monochromatization results in a pronounced peak narrowing, as is obvious from the two corresponding analyser diffraction scans shown in Figs. 4b and 4c. A quantitative analysis of the peak narrowing requires a detailed analysis of the double surface-scattering of the He beam. We therefore developed a molecular-beam tracing formalism for multiple surface-scattering experiments [12]. A detailed simulation of the experiment reveals that the measured peak narrowing agrees perfectly with the theoretical prediction. In the present geometry a monochromatization of  $\Delta\lambda/\lambda = 0.6\%$  is achieved.

The attainable resolution in the double scattering experiment is not only determined by the angular resolution of the experiment, but also depends crucially on the finite mosaic spread of the Pt crystal. Even the best available single crystals have a finite mosaic structure, i.e. the crystal consists of crystallites ( $\sim 10$ – $100$   $\mu\text{m}$ ) with slightly differing orientations. This distribution of lattice plane orientations partially cancels out the spatial wavelength separation furnished by the diffraction process. The Pt(997) crystals used in the monochromatization experiment had mosaic spreads of  $< 0.02^\circ$  (monochromator) and  $\sim 0.13^\circ$  (analyser). The large mosaic spread of the latter is the reason why the detectable monochromatization was limited to about  $5 \times 10^{-3}$  in the present experiment (note that the larger width of the monochromatized beam in Fig. 4c compared to Fig. 4b is solely due

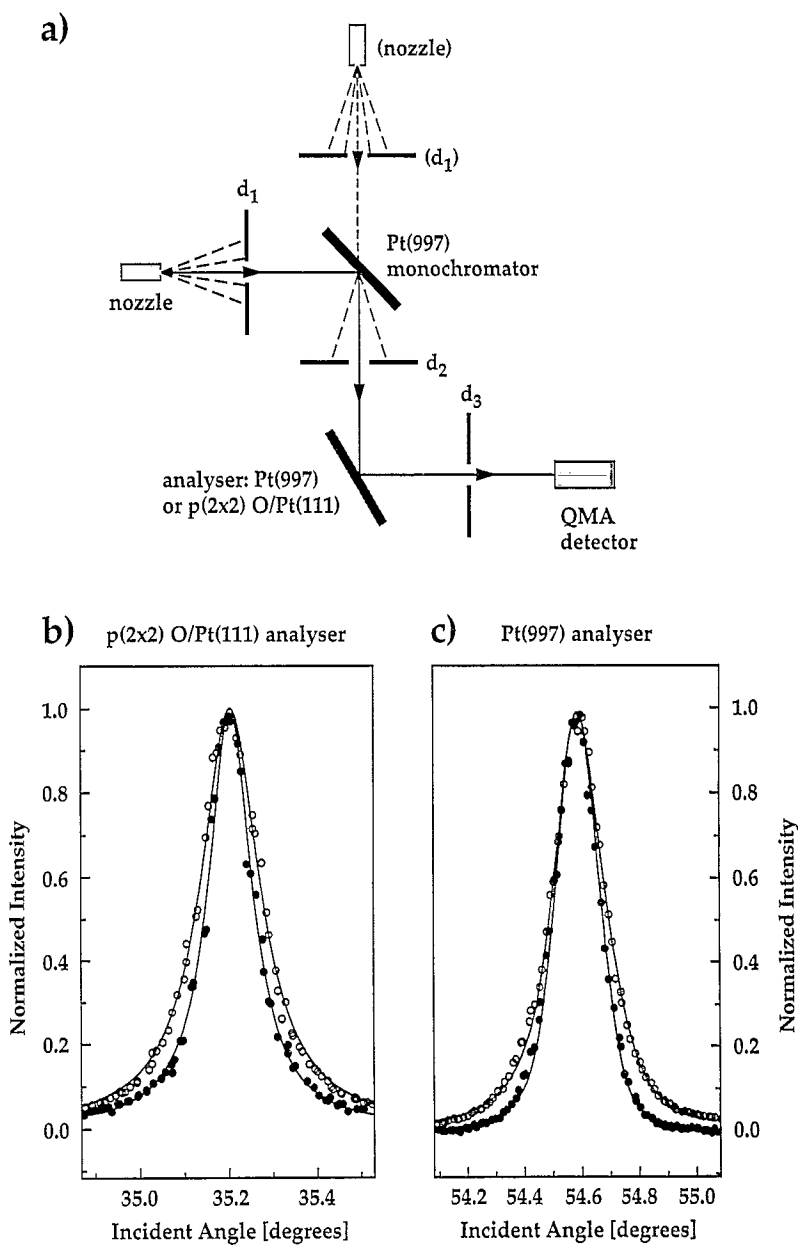


Fig. 4. (a) Geometry of the double surface scattering experiment for monochromatization (the monochromator crystal is mounted on a six-axis manipulator and can be retracted from the beam path). (b, c) High-resolution He diffraction scans ( $\lambda = 1.01 \text{ \AA}$ ) from the analyser surface with (●) and without (○) monochromatization. In (b) the  $p(2 \times 2)\text{-O-Pt}(111)$  surface has been used as the analyser, while in (c) a second  $\text{Pt}(997)$  surface has been used.

to the  $0.13^\circ$  mosaic spread of the  $\text{Pt}(997)$  analyser crystal). These resolution limitations can, however, be overcome in the future. An extensive annealing of the Pt crystal a little below the melting temperature can reduce the grown-in dislocation density

by two orders of magnitude. Indeed,  $\text{Pt}(111)$  crystals with mosaic spreads as low as  $0.003^\circ$  have already been prepared [17]. With this improved crystal preparation, wavelength resolutions of the order of  $10^{-4}$ – $10^{-3}$  will become accessible.

**References**

- [1] C.S. Adams, M. Sigel and J. Mlynek, Phys. Rep. 240 (1994) 143.
- [2] O. Stern, Naturwiss. 17 (1929) 391;  
F. Knauer and O. Stern, Z. Phys. 53 (1929) 779.
- [3] T. Engel and K.H. Rieder, Springer Tracts in Modern Physics, Vol. 91 (Springer, Berlin, 1982);  
E. Hulpke, Ed., Helium Atom Scattering from Surfaces (Springer, Berlin, 1991).
- [4] O. Carnal et al., Phys. Rev. Lett. 67 (1991) 3231.
- [5] D.W. Keith et al., Phys. Rev. Lett. 66 (1991) 2693.
- [6] B.F. Mason and B.R. Williams, Rev. Sci. Instrum. 49 (1978) 897.
- [7] E. Hecht, Optics (Addison-Wesley, Reading, MA, 1990).
- [8] G. Comsa et al., Surf. Sci. 89 (1979) 123.
- [9] E. Hahn et al., Phys. Rev. Lett. 72 (1994) 3378.
- [10] B. Poelsema et al., Surf. Sci. 117 (1982) 50.
- [11] K. Kuhnke et al., Surf. Sci. 272 (1992) 118.
- [12] H. Schief et al., to be published.
- [13] L.K. Verheij, B. Poelsema and G. Comsa, Surf. Sci. 162 (1985) 858.
- [14] A detailed discussion on the angular resolution function  $\Delta\theta$  can be found in: G. Comsa, Surf. Sci. 81 (1979) 57.
- [15] I. Estermann, R. Frisch and O. Stern, Z. Phys. 73 (1931) 348.
- [16] K. Kern et al., Phys. Rev. Lett. 56 (1986) 2064.
- [17] A.R. Sandy et al., Phys. Rev. Lett. 68 (1992) 2192.